Drug Design, Development and Therapy

Dovepress
open access to scientific and medical research

Open Access Full Text Article

ORIGINAL RESEARCH

Nano-Graphene Oxide-supported APTES-Spermine, as Gene Delivery System, for Transfection of pEGFP-p53 into Breast Cancer Cell Lines

This article was published in the following Dove Press journal:
Drug Design, Development and Therapy

Vida Mirzaie[1]
Mehdi Ansari[2,3]
Seyed Noureddin Nematollahi-Mahani[1]
Mahshid Moballegh Nasery[3]
Behzad Karimi[4]
Touba Eslaminejad[3]
Yaghoub Pourshojaei[5]

[1]Department of Anatomy, Afzalipour School of Medicine, Kerman University of Medical Sciences, Kerman, Iran; [2]Department of Drug and Food Control, Faculty of Pharmacy, Kerman University of Medical Sciences, Kerman, Iran; [3]Pharmaceutics Research Centre, Institute of Neuropharmacology, Kerman University of Medical Sciences, Kerman, Iran; [4]Surface Coating and Corrosion Department, Institute for Color Science and Technology, Tehran, Iran; [5]Department of Medicinal Chemistry, Faculty of Pharmacy and Pharmaceutics Research Center, Kerman University of Medical Sciences, Kerman, Iran

Purpose: Genetic diseases can be the result of genetic dysfunctions that happen due to some inhibitory and/or environmental risk factors, which are mostly called mutations. One of the most promising treatments for these diseases is correcting the faulty gene. Gene delivery systems are an important issue in improving the gene therapy efficiency. Therefore, the main purpose of this study was modifying graphene oxide nanoparticles by spermine in order to optimize the gene delivery system.

Methods: Graphene oxide/APTES was modified by spermine (GOAS) and characterized by FT-IR, DLS, SEM and AFM techniques. Then pEGFP-p53 was loaded on GOAS, transfected into cells and evaluated by fluorescent microscopy and gene expression techniques.

Results: FT-IR data approved the GOAS sheet formation. Ninety percent of the particles were less than 56 nm based on DLS analysis. SEM analysis indicated that the sheets were dispersed with no aggregation. AFM results confirmed the dispersed structures with thickness of 1.25±0.87 nm. STA analysis showed that GOAS started to decompose from 400°C and was very unstable during the heating process. The first weight loss up to 200°C was due to the evaporation of absorbed water, the second one observed in the range of 200–550°C was assigned to the decomposition of labile oxygen- and nitrogen-containing functional groups, and the third one above 550°C was attributed to the removal of oxygen functionalities. In vitro release of DNA demonstrated the efficient activity of the new synthesized system. Ninety percent of the cells were transfected and showed the GFP under fluorescence microscopy, and *TP53* gene was expressed 51-fold in BT-20 cells compared to β-actin as the reference gene. Flow cytometry analysis confirmed the apoptosis of the cells rather than necrosis.

Conclusion: It could be concluded that the new synthesized structure could transfer a high amount of the therapeutic agent into cells with best activity.

Keywords: DNA carrier, in vitro, gene transfer, conjugated polymer, MCF-7 cells, nanomedicine

Introduction

Gene dysfunction is the most important reason of the genetic diseases. Dysfunctions may happen due to the inhibitory and/or environmental risk factors eg magnetic force, electrical force and air, water or food pollution.[1] The broken gene with modified composition (mutated DNA), could transfer between

Correspondence: Touba Eslaminejad
Email t_eslami@kmu.ac.ir

Yaghoub Pourshojaei
Tel +983431325243
Email y.pourshoja@kmu.ac.ir

submit your manuscript | www.dovepress.com
DovePress
http://doi.org/10.2147/DDDT.S251005

generations and cause genetic diseases like cancers. Mutations in genes that control cell differentiation, proliferation and cellular homeostasis cause cancer.[2] Oncogenes and tumor suppressor genes are two categories of these genes and tumorigenesis is the consequence of oncogenes' overexpression and tumor suppressors' loss. Therefore, targeting oncogenes and tumor suppressors is one of the effective methods in the treatment of cancers.[3] The use of gold in cancer therapy sciences is to ruin the cancerous cells, so transfecting the targeted genes into cells in the form of RNA or DNA is responsive.[4] The most important tumor suppressor gene is *p53*, which is known as the guardian of the cells. Dysfunction of *p53* cause unregulated cell division and forms tumor cell mass. Hence, transfecting this gene into the cells can promote the apoptosis process and reduce the tumor.[5] Alternatively, transfecting genes into the cells needs a delivery system, that could protect the gene from the nuclease enzymes that exist in the cytoplasm.[6] An efficient delivery system should be able to carry a large amount of therapeutic agent, pass through the cell membrane easily, protect the agent from cytoplasmic enzymes, and finally throw that into nucleus baskets.[7] Lipids are the pioneer natural compounds in drug delivery, the commercial form of which are presented as Lipofectamine™. Polysaccharides like chitosan, starch and cyclodextrin are used too much because of their low price and easy access.[8] Metal core and graphene sheets are also going to be used more as targeting agents because of their capacity to load the drug and their potential in response to the external force.[6] They could also release the therapeutic agents in the targeted site. Recently we developed a pullulan/spermine/magnetic iron oleate dual-functioned composite for high-efficiency gene delivery compared to Lipofectamine™ reagent. It exhibited about 90% of transfection efficiency with enhanced green fluorescent protein (EGFP) in U87 cells.[3] In another study chitosan nanoparticles were used as the carrier compared to electroporation and Lipofectamine™. It was indicated that chitosan nanoparticles could transfect more than 90% into U87 cells.[7] In this study, due to the high shipping capacity of the graphene oxide sheets, they were used to deliver the *TP53* gene into the breast cancer cell lines. To reach this goal, graphene oxide sheets were grafted by spermine to increase the amine (NH^{2+}) groups. Amine groups act as reagent groups to bond with double-stranded DNA (dsDNA) as therapeutic agents. Therapeutic agent includes two indicators (EGFP) and reporter (neuR) and therapeutic gene (*TP53*). Then the ability of the new structure on the cell lines was evaluated by using fluorescent microscopy and real-time PCR technique.

Materials and Methods

3-aminopropyltriethoxysilane (APTES) was purchased from Sigma-Aldrich Co. (St Louis, MO, USA). DMEM, PBS, penicillin/streptomycin, and trypsin were purchased from Gibco (Thermo Fisher Scientific, Waltham, MA, USA). FBS was obtained from Hangzhou Sijiqing Biological Engineering Materials Co., Ltd (Hangzhou, China). Thiazolyl blue tetrazolium bromide (MTT) cell viability dye and dimethyl sulfoxide (DMSO) were purchased from Sigma-Aldrich. ApoflowEXFITC® kit was purchased from Miltenyi Biotec. RNX-Plus® reagent, Easy™ cDNA synthesis kit and SinaSYBER blue reaction mix without lowROX were obtained from Cinnagen (Tehran, Iran) and Parstous and SinaClon, respectively. Lipofectamine™ 2000 reagent was purchased from Invitrogen Corporation (Thermo Fisher Scientific, Waltham, MA, USA). All materials used in this study were of an analytical grade. The construction of the pEGFP-*p53* vector (5.89 kb) coding for the EGFP, which contained the tumor protein *p53* gene, was undertaken based on methods described earlier.[6] Human breast cancer cell lines MCF-7 and BT-20 were purchased from the Pasteur Institution, Tehran, Iran.

GO-APTES Sheets Synthesis

Graphene oxide was donated from a previous study.[9] GOA was prepared as described previously with a little modification.[10] Briefly, 2 g of GO was dispersed in 50 mL of ethanol along with 3 g APTES and 2 g potassium hydrogen carbonate as nucleophile and catalyst agent, respectively in a round-bottom flask and then refluxed for 8 h while magnetic stirring. The reaction was then cooled and filtrated under vacuum. Obtained GOA product was washed with distilled water and ethanol to remove the catalyst and excess APTES. In the next step, GOA was dried at 55°C in a vacuum oven, and ground into powder for later experiments (Figure 1).

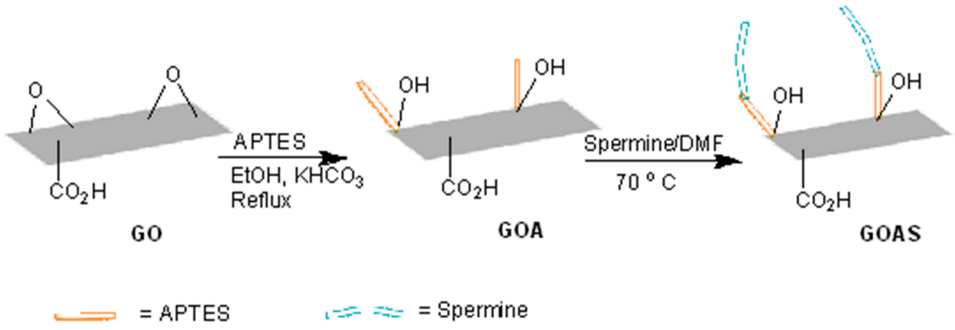

Figure 1 Schematic representation of step-by-step formulation of APTES-graphene oxide composite.

Amino-Functionalized of APTES-GO Sheets

For preparation of GOAS (graphene oxide-APTES-spermine), 30 mg of GOA along with 10 mL DMF as a solvent was added to a two-neck round-bottom flask supported with dropping funnel under inert atmosphere. Afterward 435 mg of dissolved spermine in 5 mL DMF was added to reaction mixture by means of dropping funnel drop-wise and then the mixture was stirred for 24 h at 70°C. The final product was filtered and washed with ethanol several times and dried under vacuum (Figure 1).

Loading of pEFGP-p53 on GOAS Sheets

EFGP-p53 plasmid (5%; w/w) was added to the GOAS drop-wise and incubated at room temperature for 50 min and then was stored in the refrigerator (4 °C).

Physical Characterization of Nanoparticles

FT-IR spectra of GO, APTES, SP, GOA, and GOAS were recorded as KBr discs in the 500–3500 cm^{-1} range on Bruker Optics' RockSolid™ design. The powder sample and KBr must be ground to reduce the particle size of less than 5 mm in diameter because the large particles scatter the infrared beam and cause a slope baseline of the spectrum. Parameters such as size of particles and zeta potential were measured using a kinetic nanoparticle size analyzer VASCO KIN™ (Cordouan Technologies, Pessac, France). The surface and cross sectional morphology of the GOAS (sonicated) were analyzed using field emission scanning electron microscopy (FE-SEM, MIRA 3 XM, Tescan USA Inc.) after sputter coating with gold for five minutes. All samples were examined at an acceleration voltage of 15 kV. The shape and surface topology was characterized using atomic force microscope (AFM) (Bio7-AFM, Arapajohesh, Iran) instrument. Briefly, 500 µL of each sample was placed on freshly cleaved mica sheet and incubated at room temperature till dried. The section analysis and the peak height of particles for 3D images were analyzed using Imager Ara Analysis software. The content of GO in the GOAS was determined by using a BAHR STA 503 thermoanlyzer. Samples of GOAS nanoparticles weighing between 5 and 15 mg were heated in air from 10 to 800°C at a heating rate of 10°C/min.

Gel Retardation Assay

The bonding of plasmids to complexes was studied by agarose gel electrophoresis run for 30 min at 100 V (Sub-Cell GT 96/192, Bio-Rad Laboratories Inc., (Hercules, CA, USA), followed by DNA green viewer staining (Parstous). GOAS/pEGFP-p53 (5 mg) was prepared in 1 mL of 10 mM PBS solution and incubated for 15 min, then the complexes (1 µL) were mixed with loading buffer (0.1% sodium dodecyl sulfate, 5% glycerol, and 0.005% bromophenol blue) and run on an agarose gel (2%). The gel was imaged with Kodak Image Station.

Nuclease Resistance Assay

To investigate the ability of the copolymer to protect DNA from enzymatic degradation, 3 µL of GOAS/pEGFP-p53 (containing 0.75 µg plasmids) and pEGFP-p53 (control) were combined with DNase I (2 U) in 4 µL 50 mM Tris–HCl at pH 7.4, separately. After incubation for 1 h at 37°C, samples were run on an agarose gel and visualized using a UV image capture system. Naked plasmid (pEGFP-p53) was served as a positive control.

Determination of Release Profile

To quantify the DNA release from the nanostructured systems, 2 mL of GOAS/pEGFP-p53 (2 mg/mL) were

incubated in PBS (pH 7.4, 37°C) with gentle magnetic stirring for 72 h. Samples were centrifuged (16,000 g; 10 min) and the supernatant was removed and replaced with 2 mL of fresh PBS, divided into five tubes and incubated at room temperature (initial concentration of DNA for each time point was 20 μg). At fixed time points (5, 9, 18, 23, 30 days); supernatant was collected and quantified by NanoDrop™ 2000 Spectrophotometer. Furthermore, the released DNA from the samples was assessed by running on the gel and compared with control (pure pEGFP-p53). All measurements were carried out in triplicate.

Cell Culture and Cytotoxicity Assay

MCF-7 and BT-20 cells were cultured in DMEM-F12 supplemented with 10% FBS and were maintained in a humidified incubator with 5% CO_2 at 37°C. Cytotoxicity of GOAS and GOAS/pEFGP-p53 complexes was assessed by MTT assay according to the manufacturer's protocol. Cells were collected and seeded in 96-well plates with a density of 1×10^4 cells/well and incubated for 24 h. 20 μL of different concentrations (0.001, 0.01, 0.1, 1, 10, 100 and 1000 ppm) of GOAS and GOAS/pEFGP-p53 complexes were mixed with 80 μL serum-free media and kept at room temperature for 20 min. After that, the whole 100 μL of GOAS and GOAS/pEFGP-p53 complexes were transferred into each well containing cells and incubated for four hours. Then, serum-free media were replaced by fresh media containing 10% FBS and the infected cells were incubated for more 24 h. Next day, 10 μL of MTT solution was added into each well and incubated for four hours, and 100 μL of DMSO was added into each well afterward. The absorbance was read at 570–630 nm by immune absorbent assay (ELISA) (multi-mode reader, Synergy II, Bio-tek Instruments, Winooski, VT, USA).

Transfection Methods

GOAS-pEFGP-p53 complexes were mixed with 80 μL serum-free media and kept at room temperature for 20 min. Then 200 μL of transfection complex was added to each well and mixed gently by rocking the plate back and forth. The inoculated cells were incubated for 24–72 h at 37°C; 5% CO_2 and the serum-free media were replaced with complete medium the next day. Lipofectamine™ was used as standard reagent for common delivery systems to check the plasmid DNA and experimental conditions.

Fluorometric Detection of Cellular EGFP

Transfected cells were maintained on an Olympus (TH 1400) inverted, phase-contrast fluorescent microscope up to 72 h before examination for EGFP expression. Images were recorded using attached digital imaging system.

Real Time PCR and Gene Expression

Six days after transfection, cells were lysed by adding 1 mL of RNX-Plus® reagent following the manufacturer's instructions. Proteins removed by chloroform extraction to obtain an A 260/280 ratio of 1.81±0.06. cDNA synthesis (approximately 1 μg) from total mRNA was carried out using a reverse transcriptase kit (Easy™ cDNA Synthesis Kit; Parstous). RT-qPCR was performed using the SinaSYBER blue reaction mix without lowROX (SinaClon) in a Rotor-Gene real time PCR system, using 1 μL of each cDNA sample and 10 μM of each primer. The reaction was run as follows: 95°C for seven minutes min, followed by 40 cycles of 95°C for 15 s, 65°C for 20 s, and 72°C for 35 s. In order to check the appearance of the PCR product, samples were run on gel electrophorese. The CT (threshold cycle) values were analyzed using $2^{-\Delta\Delta CT}$ methods.[11] The fold change in gene expression was normalized to endogenous reference genes (*GAPDH* and *β-actin*) and expressed relative to the untreated control. Norm finder software was used to evaluate expression stability of the candidate reference genes.

Apoptosis Assay

Cell apoptosis was assessed by flow cytometry using the ApoflowEXFITC® kit, following the manufacturer's instructions. Cells were suspended in 50 μL of binding buffer (10 mM Hepes, pH 7.4, 140 mM NaCl, 2.5 mM CaCl, 0.1% BSA), and 2.5 μL Annexin V-FITC (Miltenyi Biotec) and incubated for 15 min in the darkness. Then 430 μL of binding buffer and 1 μg/mL propidium iodide (PI) were added to the cells. Finally, the flow cytometric analysis was carried out using a FACS Calibur device (LSR II; BD Biosciences, San Jose, CA, USA) and the results were evaluated by WinMDI software (Treestar). The PI^+ cells were gated out first, while the remaining cells were assessed to determine the frequency of Annexin V^+ cells.

Statistics Analysis

Statistical comparison between treatment groups at different concentrations were investigated using one-way ANOVA by SPSS software 15 for windows (SPSS Inc., Chicago, IL, USA) ($p \leq 0.05$).

Results

Physical Characterization of Nano Sheets

The hydroxyl groups of GO structure are indistinguishable because of the large quantities of functional groups bearing OH on the surface of the sheets. The FT-IR spectrum of GO gives the possible functionalities: OH, carboxylic acid, OH alcoholic, C=O, and C-O etheric, the peaks appeared at higher than 3000 as broad peaks, 1720, and 1060 cm^{-1}, respectively. The reference spectrum was obtained for pure APTES, with the evidence of Si–O–Si, SP^3 CH and NH_2 bonds (Figure 2). FT-IR spectrum of the GOA indicated that the asymmetric and symmetric stretching vibrations of CH_2 of APTES on GO substrate appeared at 2934 and 2856 cm^{-1}. The reference peak of spermine revealed NH_2 above 3000 cm^{-1} and bending CH groups at 1500 cm^{-1} in FT-IR. The FT-IR spectrum of GOAS revealed the bands at 1651, 2934, and 3388 cm^{-1} that are characteristic peaks of carbonyl of carboxylic acid, CH of alkane chains and amine groups, respectively (Figure 2). GOAS particles were recorded by dynamic light scattering showed different measurement of 32–56 nm at room temperature (Figure 3A). Flocculation stability behavior of the GOAS solution was predicted due to zeta potential of less than ±5 (Figure 3B). PDI obtained from the distribution profile is 0.55 which indicates GOAS are monodisperse. SEM analysis of GOA functioned by spermine showed that the nanoparticles of the APTES grafted graphene oxide were dispersed in the spermine matrix as well with no aggregation. Layer-sheet structure of GO was clear in the SEM micrograph (Figure 4). The morphology and the height profiles of GOAS in the AFM images indicated dispersed structures with some aggregation (Figure 5A and B). Analysis of the height profiles from the dispersed GOAS structures revealed a thickness of 1.25±0.87 nm. STA analysis of the GOAS was done by heating the samples at a constant rate of 10°C min^{-1} from 0 to 800°C under N_2 flow. GOAS was started to decompose from 400°C and was very unstable during the heating process (Figure 6A). TG graph shows an increase from 20°C, which may be the consequence of oxidation of GOAS. The first weight loss up to 200°C, was due to the evaporation of absorbed water, carbon dioxide and other products, the second weight loss observed in

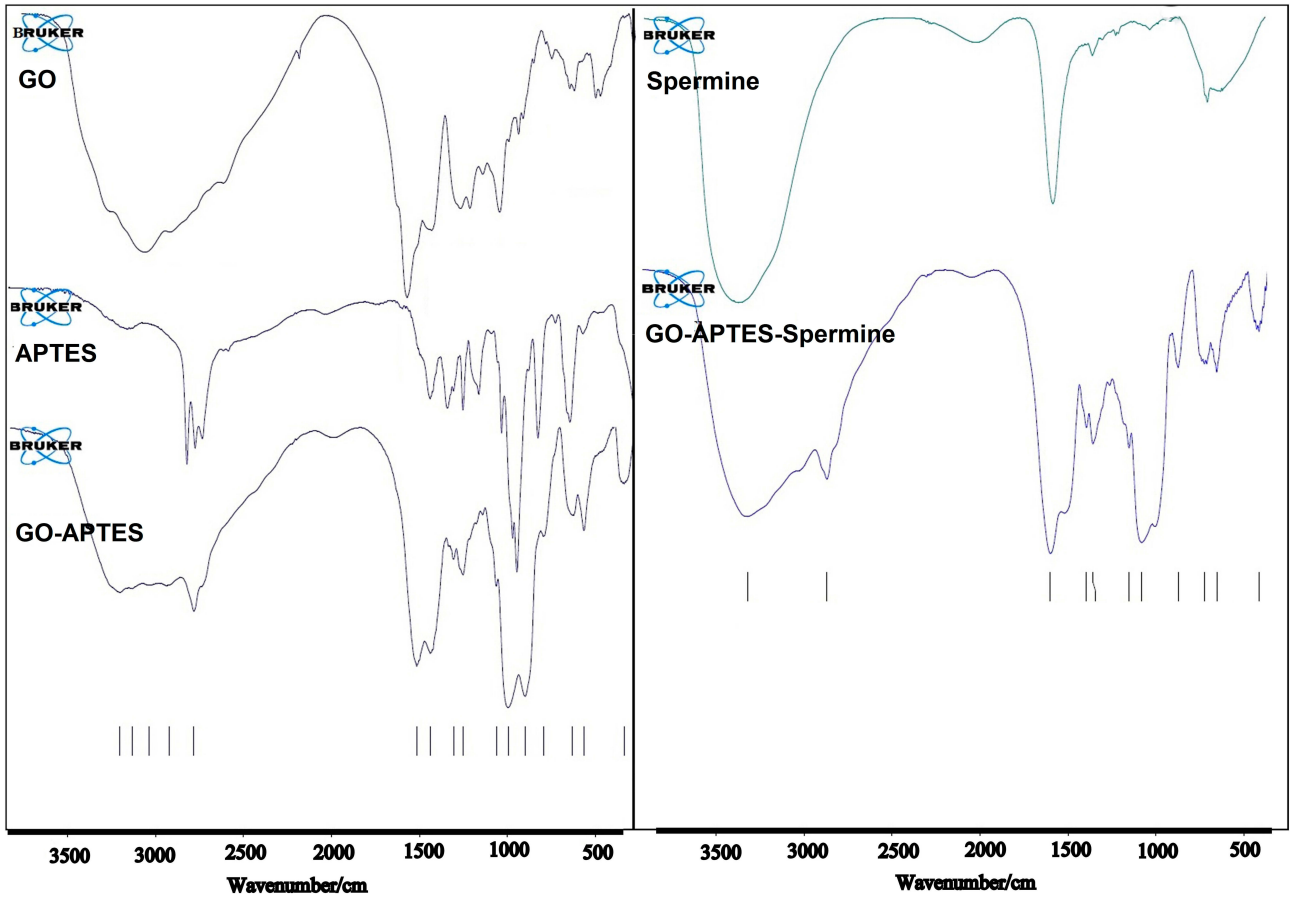

Figure 2 FTIR spectra analysis of GO, APTES and GOA, Spermine and functioning of GO-APTES by Spermine.

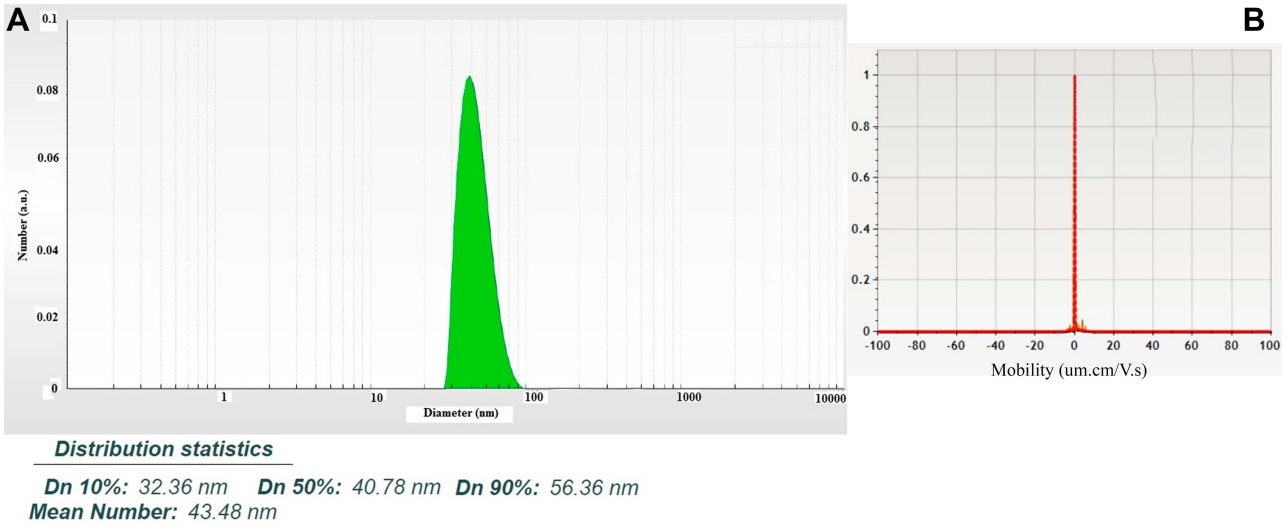

Figure 3 Particle size distribution and zeta potential of GOAS nanoparticles. (**A**) Size distribution of GOAS nanoparticles with mean diameter of 44 nm, (**B**) Zeta potential of less than ±5 showed the flocculation stability behavior of the GOAS solution.

the range of 200–550°C and was assigned to the decomposition of labile oxygen-containing functional groups, and the third weight loss above 550°C, was attributed to the removal of more stable oxygen functionalities (such as alcohol, carboxylic acids), which usually decompose at higher temperatures (Figure 6B).

Gel Retardation Assay and Nuclease Resistance Study

The data of gel retardation assay showed that the whole plasmids were bounded on or into the GOAS sheets according to no bands remaining on the gel (Figure 7A, lane c). DNase enzyme was added to GOAS/pEGFP-p53 complex in order to examine the ability of the GOAS carrier to protect the loading DNA. Electrophoresis had no smear bands on the gel (Figure 7A, lane d).

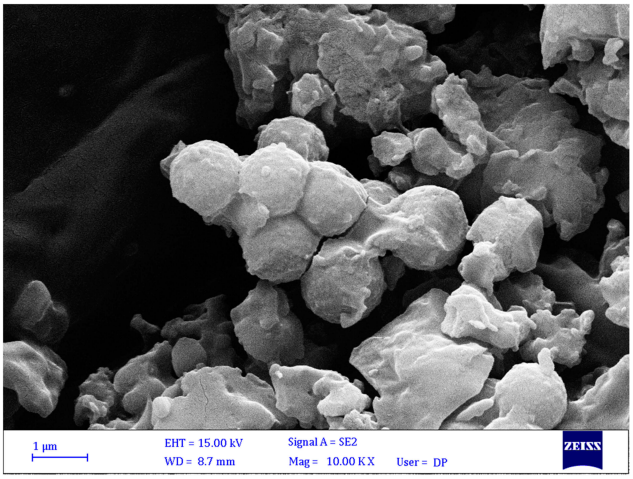

Figure 4 SEM micrographs of the synthesized particles of GOAS showed the separated sheets.

Determination of Release Profile

Concentration of the released DNA from GOAS-pEFGP-p53 complex was measured during one month and the results showed that new construction could act as a slow release structure. The initial release within the first five days was 12.4% and was on the rise during days 9, 18, and 23 (34.8, 53.6 and 68.6%, respectively) and continued to increase until day 30 (85.2%) cumulatively (Figure 7B). The DNA integrity test at fixed time points was assessed by agarose gel electrophoresis. The results revealed that there were no differences between plasmid DNA expression of the released DNA and the controlled plasmid DNA, which indicated that the DNA adsorption and release from the complex do not alter the functionality of the plasmid.

Transfection Efficiency and Gene Expression

Transfection process was validated briefly by observing transfected cells by GOAS-pEFGP-p53 complexes (Figure 8A) under a fluorescent microscope. Ninety percent of the cells showed florescence after 72 h of incubation (Figure 8B). BT cell line feature an increase of expression of *TP53* (51 folds), whereas MCF-7 cell line showed an unchanged level of mRNA copies of *TP53* compared to *β-actin* as references gene (Figure 8C).

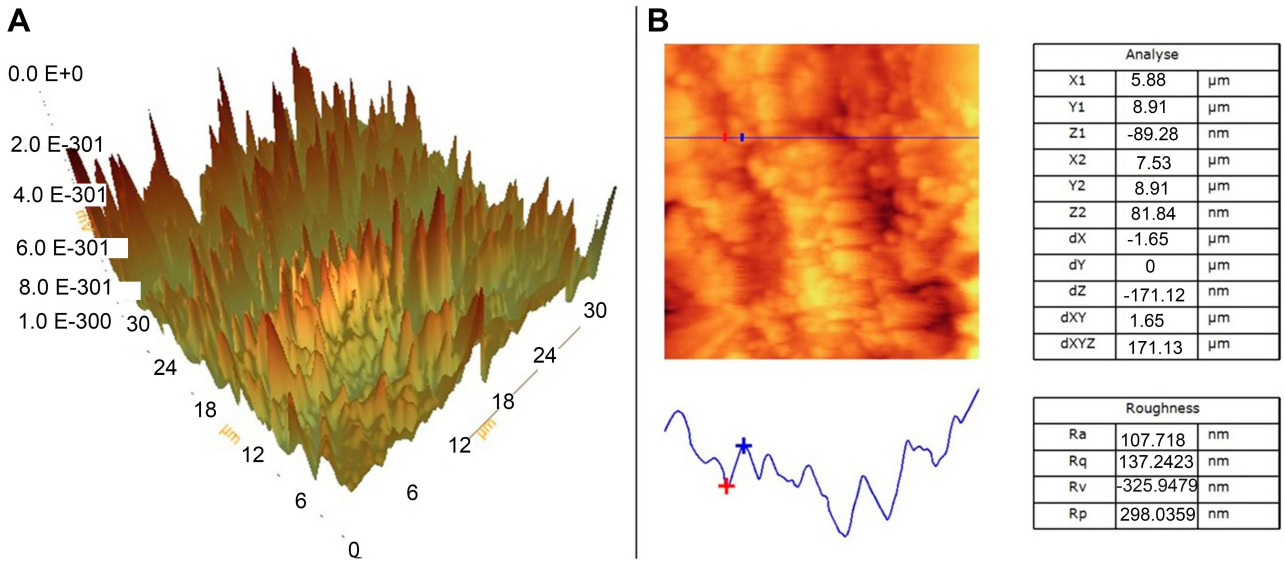

Figure 5 AFM micrograph of GOAS. (**A**) 3D topography AFM images of nanoparticles; Scale bar, 1 µm, (**B**) Section analysis of the height profiles of nanoparticles in the 2D AFM images.

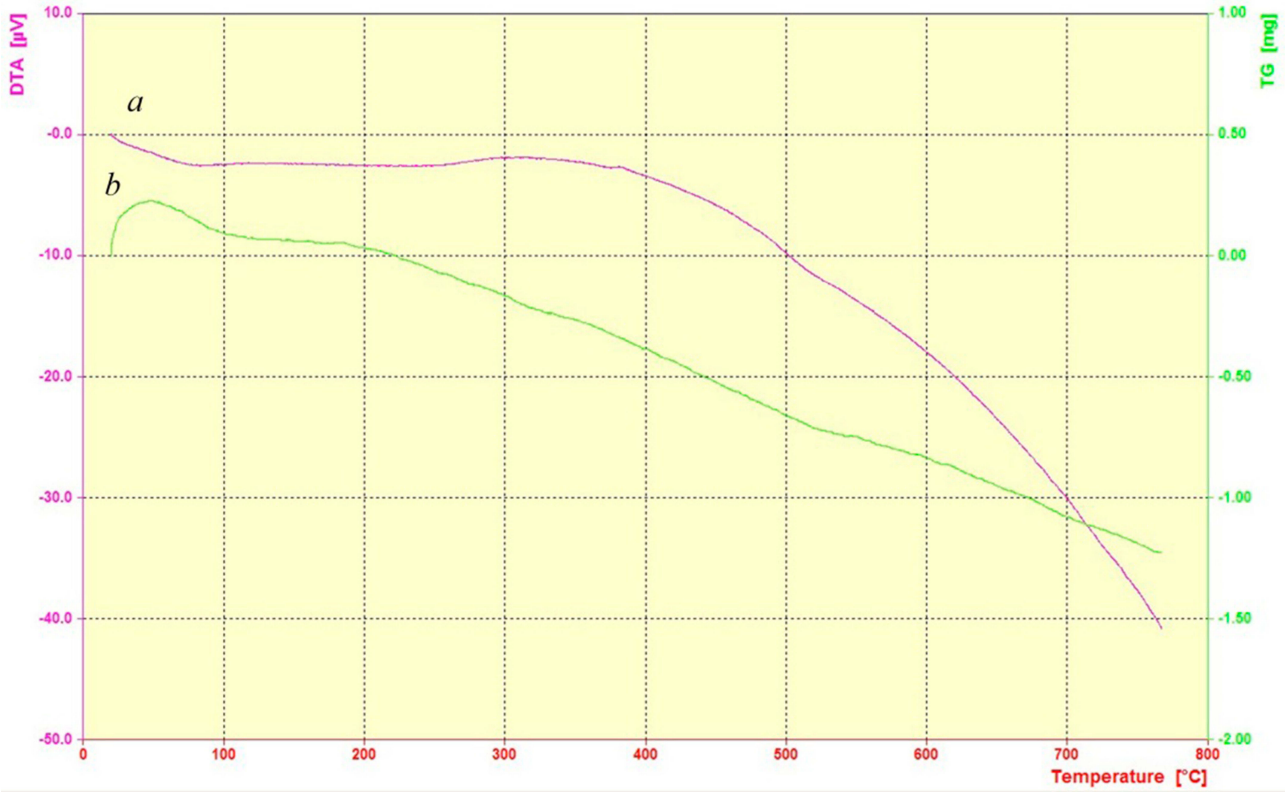

Figure 6 STA analysis of the synthesized particles of GOAS. (a) DTA analysis, (b) TG analysis.

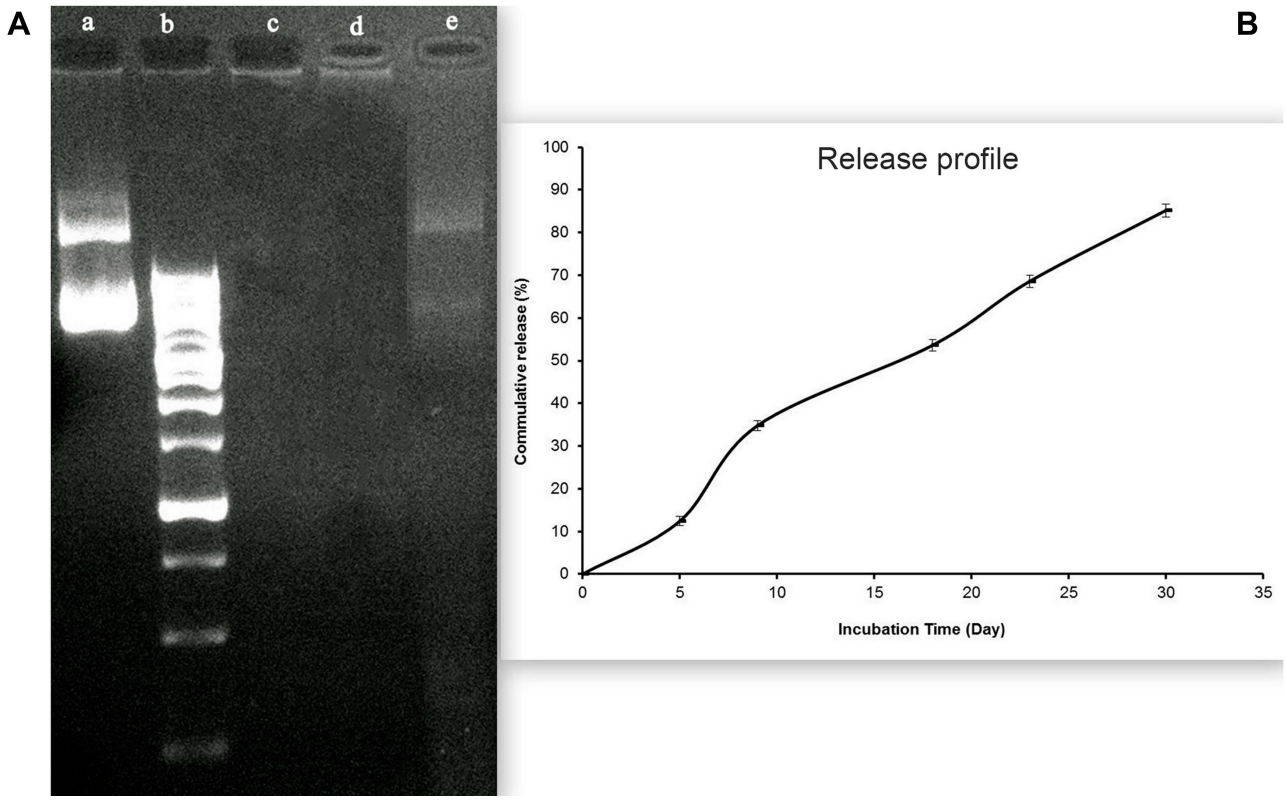

Figure 7 Gel retardation assay, nuclease resistance study and release profile of EGFP-p53 plasmid encapsulated in GOAS. (**A**) EGFP-p53 plasmid as negative control (lane a), DNA marker (lane b), GOAS-pEGFP-p53 (lane c), DNase I digested GOAS-pEGFP-p53 (lane d) and DNase I digested pEGFP-p53 plasmid as positive control (lane e), (**B**) Release profile of EGFP-p53 plasmid.

Apoptosis Assay of Nanospheres

Flow cytometry analysis results showed that almost 30% of the cells were dead through apoptosis comparing to the control cells at an LD_{50} concentration during 72 h incubation (Figure 9).

Discussion

A new drug delivery system called GOAS was prepared in this study in two steps. In the first step, GOA was obtained via nucleophilic attack of APTES nitrogen to epoxy group on the basal plane of the GO in the presence of basic media in EtOH. Carboxylic acid is less active than acidic condition in the basic media and this may cause amide formation, which is less likely to happen than ring opening in this condition. FT-IR spectrum of GOA showed the functional groups of N-C (1388 cm^{-1}), C-Si (774 cm^{-1}), Si-O (1078 cm^{-1}), C-O (1103 cm^{-1}), OH (up to 3000 cm^{-1}), and SP^3 CH (2934 cm^{-1}) that corresponded to this intermediate.[12] In the next step, GOA sheets were grafted to spermine in DMF as solvent, at 70°C to achieve the GO-supported-APTES-spermine that known as GOAS. The comparison of FT-IR spectra of GOA, spermine, and GOAS proved the reaction of spermine with GOA according to 3388 cm^{-1} peak that was attributed to amine group. Due to the amine groups on the surface of the GOAS, a high amount of DNA could attach to the GOAS and transfer into the cells. This new system was able to protect the gene from nuclease enzymes and had a high expression level of *TP53* because of its grabbing properties. The GOAS/DNA interaction via hydrogen bonds and electrostatic interactions was enhanced by the creation of the functional groups on the GO.[13] Therefore, all of the functional groups were confirmed through FT-IR analysis. DLS and zeta potential results confirmed that the synthesized GOAS particles were too small in size (60 nm) with flocculation stability behavior. According to the previous studies the size of particles plays a key role on their ability to deliver drugs into cells.[14] As it is known, the immune cells remove large objects (<300 nm) from the bloodstream.[15] Thus, cell transfection could occur on a large scale by using GOAS nanoparticles. Morphological and topological structures of the new synthesized delivery system were evaluated by using SEM and AFM. SEM

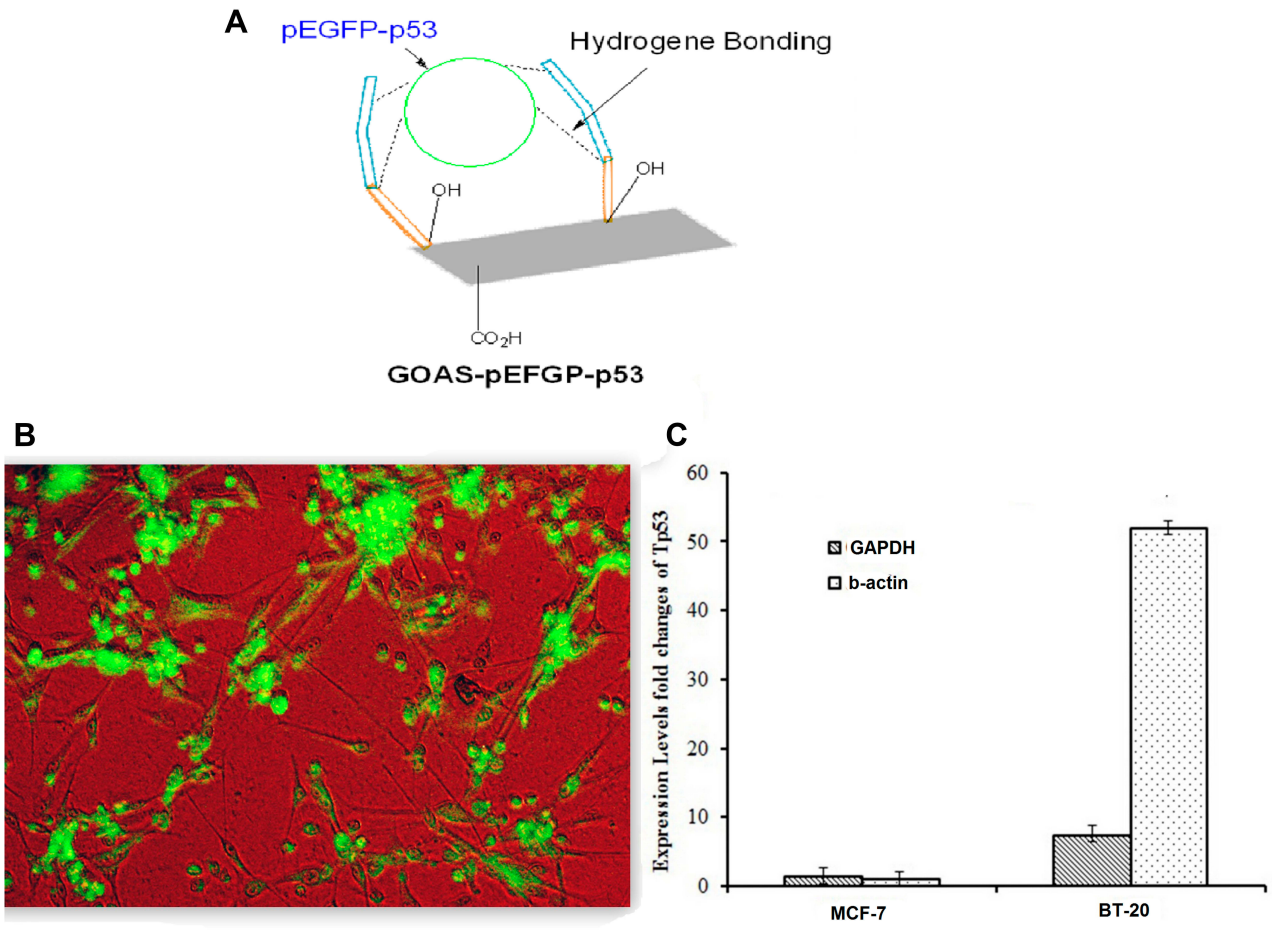

Figure 8 Schematic picture of GOAS-pEGFP-p53, micrograph of florescence cells and gene expression results were presented. (**A**) Schematic picture of GOAS-pEGFP-p53, (**B**) BT cells transfected by GOAS-pEGFP-p53, (**C**) Gene expression results of the *TP53* gene in MCF-7 and BT cell lines. Data are shown as mean ±SD; Scale bar: 200 nm.

images confirmed that the GO sheets were firmly suspended and did not bend. Our results were similar to what was described by others.[16] Dispersed sheets of the GOAS confirmed the synthesis procedure. AFM micrograph emphasizes the fine topology of the synthesized sheets and 3D topography showed different phases with different colors that means GOA were grafted to spermine as well.[17] Simultaneous thermal analysis approved that the newly synthesized sheets were unstable during the heating process because of different functionalities. This instability may be due to the more uniform population of oxygen functionalities on the graphene oxide surface and a higher concentration of carboxylic acid functionalities.[18] Biophysical characteristics of the GOAS-pEGFP-*p53* that were evaluated by gel retardation, nuclease resistance and in vitro release confirmed that GOAS has the ability to protect DNA from nuclease enzymes and also has more capacity to carry DNA as a therapeutic agent.[19] The absence of smear in lane c (Figure 7A), leads to the hypothesis that there are strong electrostatic interactions between GOAS and DNA, at least under these experimental conditions. Lane d in agarose gel electrophoresis and no migration of free DNA indicating that most of the DNA was captured by the nanoparticles because of the high affinity of spermine to the DNA.[20] Indeed, it is known that a strong electrostatic interaction exists between the phosphate groups of DNA and the amino groups of spermine, as well as hydrophobic and hydrogen bonds.[21] Nanoparticles stability and nucleic acid protection are important parameters for efficient nucleic acid delivery.[22] Release profiles of nanoparticles made with GOAS-pEGFP-p53 incubated in PBS showed that these structures were able to release DNA constantly over 30 days. Evaluating the ability of the GOAS-pEGFP-p53 system to transfect into animal cells using fluorescent technique, gene expression and flow cytometry analysis revealed that more than 90% of the cells were fluorescence, which means the reporter gene could act as well. The therapeutic

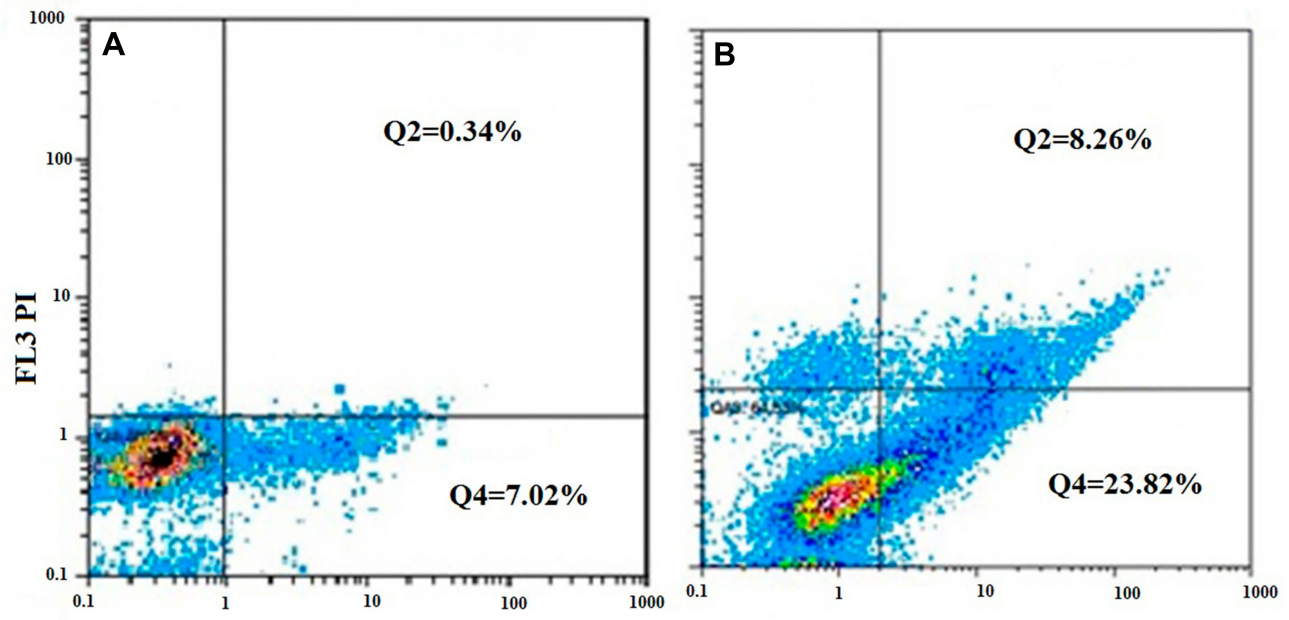

Figure 9 Apoptosis analysis of the transfected cells by LD_{50} dose of the GOAS-pEGFP-p53 on cells compare to control. (**A**) Control. (**B**) Treated cells.

gene (*TP53*) also showed an increased expression compared to *β-actin* as references gene in BT cells. Graphene oxide nano carriers that were used to internalizes into HeLa cells showed more than 70% fluorescence.[23] In another study, graphene oxide functionalized with polyethyleneimine (PEI-GO) was indicated as an effectively delivery plasmid DNA into cells that be localized in the nucleus.[24] Graphene oxide nanocarriers was designed by modification of a folic acid and β-cyclodextrin to improve its specialty characteristics to uptake into cells.[25] Also in a study, the delivery of doxorubicin and D-α-Tocopherol succinate by PEGylated graphene oxide to cancer cells induced a stronger therapeutic effect than that attained with the free drug combination.[26] The expression level of the *TP53* in MCF-7 cell line was less than BT cells, which may be because of some inhibitors that may exist inside the MCF-7 cells that inhibit the *TP53* expression.[27] Flow cytometry assay showed an apoptosis in the cells that confirm the new synthesized delivery system was able to transfer the therapeutic agent into the cells in a healthy way and large amount.

Conclusion

In this study, a new drug delivery system was synthesized during two steps containing silanization and amination of GO with APTES and spermine, respectively. According to the results, it could be concluded that the new synthesized delivery system was able to transfer a large amount of the therapeutic agent into the cells properly. Thereafter, it could be used as a new promising delivery system to transfer genes or drugs into targeted cells, especially cancer cells. The new delivery system indicated that it could transfect into cells easily because it is well structured and small in size.

Acknowledgment

This research received a specific grant from Kerman University of Medical Sciences under project no. 96000748. The authors would like to give special thanks to Kerman University of Medical Sciences because of its spiritual and ethical support.

Disclosure

The authors report no conflicts of interest in this work.

References

1. Pacheco I, Buzea C, Tron V. Towards new therapeutic approaches for malignant melanoma. *Expert Rev Mol Med*. 2011;13:e33. doi:10.1017/S146239941100202X
2. Vogelstein B, Kinzler KW. Cancer genes and the pathways they control. *Nat Med*. 2004;10(8):789. doi:10.1038/nm1087
3. Eslaminejad T, Noureddin Nematollahi-Mahani S, Ansari M. Glioblastoma targeted gene therapy based on pEGFP/p53-loaded superparamagnetic iron oxide nanoparticles. *Curr Gene Ther*. 2017;17(1):59–69. doi:10.2174/1566523217666170605115829

4. Pan L, Liu J, Shi J. Cancer cell nucleus-targeting nanocomposites for advanced tumor therapeutics. *Chem Soc Rev*. 2018;47(18):6930–6946. doi:10.1039/C8CS00081F
5. Aubrey BJ, Kelly GL, Janic A, Herold MJ, Strasser A. How does p53 induce apoptosis and how does this relate to p53-mediated tumour suppression? *Cell Death Differ*. 2018;25(1):104. doi:10.1038/cdd.2017.169
6. Eslaminejad T, Nematollahi-Mahani SN, Ansari M. Synthesis, characterization, and cytotoxicity of the plasmid EGFP-p53 loaded on pullulan–spermine magnetic nanoparticles. *J Magn Magn Mater*. 2016;402:34–43. doi:10.1016/j.jmmm.2015.11.037
7. Eslaminejad T, Nematollahi-Mahani SN, Ansari M. Cationic β-cyclodextrin–chitosan conjugates as potential carrier for pmCherry-C1 gene delivery. *Mol Biotechnol*. 2016;58(4):287–298. doi:10.1007/s12033-016-9927-0
8. Kumari RM, Sharma N, Gupta N, Chandra R, Nimesh S. Synthesis and evolution of polymeric nanoparticles: development of an improved gene delivery system. In: Grumezescu AM, editor. *Design and Development of New Nanocarriers*. Elsevier; 2018:401–438.
9. Miraftab R, Karimi B, Bahlakeh G, Ramezanzadeh B. Complementary experimental and quantum mechanics approaches for exploring the mechanical characteristics of epoxy composites loaded with graphene oxide-polyaniline nanofibers. *J Ind Eng Chem*. 2017;53:348–359. doi:10.1016/j.jiec.2017.05.006
10. Serodre T, Oliveira NA, Miquita DR, et al. Surface silanization of graphene oxide under mild reaction conditions. *J Braz Chem Soc*. 2019;30(11):2488–2499.
11. Livak KJ, Schmittgen TD. Analysis of relative gene expression data using real-time quantitative PCR and the 2−ΔΔCT method. *Methods*. 2001;25(4):402–408. doi:10.1006/meth.2001.1262
12. Kim Y, Park H, Kim B. Triple shape-memory effect by silanized polyurethane/silane-functionalized graphene oxide nanocomposites bilayer. *High Perform Polym*. 2015;27(7):886–897. doi:10.1177/0954008314565398
13. Hu Y, Li F, Bai X, et al. Label-free electrochemical impedance sensing of DNA hybridization based on functionalized graphene sheets. *Chem Comm*. 2011;47(6):1743–1745. doi:10.1039/C0CC04514D
14. Pinelli F, Perale G, Rossi F. Coating and functionalization strategies for nanogels and nanoparticles for selective drug delivery. *Gels*. 2020;6(1):6. doi:10.3390/gels6010006
15. Giulimondi F, Digiacomo L, Pozzi D, et al. Interplay of protein corona and immune cells controls blood residency of liposomes. *Nat Commun*. 2019;10(1):1–11. doi:10.1038/s41467-019-11642-7
16. Alam SN, Sharma N, Kumar L. Synthesis of graphene oxide (GO) by modified hummers method and its thermal reduction to obtain reduced graphene oxide (rGO). *Graphene*. 2017;6(1):1–18. doi:10.4236/graphene.2017.61001
17. Ghanem A, Abdel Rehim M. Assisted tip sonication approach for graphene synthesis in aqueous dispersion. *Biomedicines*. 2018;6(2):63. doi:10.3390/biomedicines6020063
18. Nováček M, Jankovský O, Luxa J, et al. Tuning of graphene oxide composition by multiple oxidations for carbon dioxide storage and capture of toxic metals. *J Materi Chem A*. 2017;5(6):2739–2748. doi:10.1039/C6TA03631G
19. Liu Y, Liu Z, Wang Y, et al. Investigation of the performance of PEG–PEI/ROCK-II-siRNA complexes for alzheimer's disease in vitro. *Brain Res*. 2013;1490:43–51. doi:10.1016/j.brainres.2012.10.039
20. Molnar MM, Liddell SC, Wadkins RM. Effects of polyamine binding on the stability of DNA i-motif structures. *ACS Omega*. 2019;4(5):8967–8973. doi:10.1021/acsomega.9b00784
21. Shen Z-L, Xia Y-Q, Yang Q-S, Tian W-D, Chen K, Ma Y-Q. Polymer–nucleic acid interactions. *Top Curr Chem*. 2017;375(2):44. doi:10.1007/s41061-017-0131-x
22. Zhou S, Chen W, Cole J, Zhu G. Delivery of nucleic acid therapeutics for cancer immunotherapy. *Med Drug Discov*. 2020;6:100023. doi:10.1016/j.medidd.2020.100023
23. Campbell E, Hasan MT, Pho C, Callaghan K, Akkaraju GR, Naumov AV. Graphene oxide as a multifunctional platform for intracellular delivery, imaging, and cancer sensing. *Sci Rep*. 2019;9(1):416. doi:10.1038/s41598-018-36617-4
24. Chen B, Liu M, Zhang L, Huang J, Yao J, Zhang Z. Polyethylenimine-functionalized graphene oxide as an efficient gene delivery vector. *J Mater Chem*. 2011;21(21):7736–7741. doi:10.1039/c1jm10341e
25. Ye Y, Mao X, Xu J, Kong J, Hu X. Functional graphene oxide nanocarriers for drug delivery. *Int J Polym Sci*. 2019;2019:8453493. doi:10.1155/2019/8453493
26. de Melo-diogo D, Costa EC, Alves CG, et al. POxylated graphene oxide nanomaterials for combination chemo-phototherapy of breast cancer cells. *Eur J Pharm Biopharm*. 2018;131:162–169. doi:10.1016/j.ejpb.2018.08.008
27. Cui Q, Jh YU, Jn WU, et al. P53-mediated cell cycle arrest and apoptosis through a caspase-3-independent, but caspase-9-dependent pathway in oridonin-treated MCF-7 human breast cancer cells. *Acta Pharmacol Sin*. 2007;28(7):1057–1066. doi:10.1111/j.1745-7254.2007.00588.x